

Numerical solution of the general high-dimensional multi-term time-space-fractional diffusion equations

Xiaogang Zhu*

School of Science, Shaoyang University, Shaoyang, 422000, P.R. China

Abstract

In this article, an advanced differential quadrature (DQ) approach is proposed to obtain the numerical solutions of the two- and three-dimensional multi-term time-space-fractional diffusion equation (TSFDE) on general domains. The fractional derivatives in space are firstly discretized by deriving a new class of differential quadrature (DQ) formulas with radial basis functions (RBFs) being the trial functions. Then, the original problems are converted to a group of multi-term fractional ordinary differential equations (ODEs), which are further treated by a class of high-order difference schemes based on the weighted and shifted Lubich difference operators. The presented DQ method is high accurate and convergent on arbitrary domains. Finally, several numerical examples are carried out to illustrate its accuracy and effectiveness.

Keywords: radial basis functions, differential quadrature, multi-term time-space fractional diffusion equation.

1. Introduction

During the last ten years, fractional calculus came into the focus of interest in academic circles as an important branch of mathematics. Due to its non-locality and self-similarity, it has been proven to be very adequate to describe the dynamics phenomena with long term memory memory and hereditary effects like the anomalous transport in complex heterogeneous aquifer [1]. The application of fractional calculus has been very extensive recently, including biology, chemistry, physics, economics, and many other disciplines.

The fractional partial differential equations (PDEs) are the results of mathematical modelling based on fractional calculus, which provides a new powerful tool for the study of mathematical physics or even for the whole scientific research. Nevertheless, there raises a challenge to solve these type of equations and few of fractional PDEs can be solved by analytic techniques. As an result, numerical methods are clearly a priority for development. Until now, the numerical algorithms for the time-fractional PDEs is on the way to maturity after recent years' development [26, 33, 23, 43, 39, 46, 19, 20], while these for high-dimensional space-fractional PDEs have to be further developed and advanced, especially for the ones defined on general domains. Regardless of the difficulties in constructing numerical algorithms for the space-fractional PDEs, many numerical methods have been invented to solve them, covering finite difference (FD) methods [32, 40, 21, 22], spectral methods [5, 44], finite element (FE) methods [15, 13, 45, 47], and finite volume methods [44, 29]. Liu et. al considered a space-fractional FitzHugh-Nagumo monodomain model by an implicit semi-alternative direction FD scheme on approximate irregular domains [28]. Qiu et al. considered a nodal discontinuous Galerkin method and solved a L-shaped domain problem [38]. Yang et.al proposed a fully discrete FE method for the two-dimensional space-fractional diffusion equation on convex domains [42]. Bhrawy and Zaky developed a spectral tau method for the multi-term time-space fractional PDEs [6]. In [11], an efficient algorithm based on FD and FE methods was addressed for the two-dimensional multi-term time-space-fractional Bloch-Torrey equations. In [16], a fully discrete FE method was given for the two-dimensional multi-term time-space fractional

*Corresponding author

Email address: zhuxg590@yeah.net (Xiaogang Zhu)

diffusion-wave equation. Although the numerical treatment of multi-term time-space-fractional PDEs is also an active area of research, few works can be found to solve these equations on general high-dimensional domains.

Meshless methods eliminate tedious mesh generation and reconstruction or only use easily generable meshes in a flexible manner, and can reduce computational cost, which serve as a promising alternative in dealing with structure destruction, high-dimensional crack propagation, and large deformation problems. Meshless methods have been achieved great progress, such as diffuse element method [34], reproducing kernel particle method [18], hp-cloud method, element-free Galerkin method [4], meshless local Petrov-Galerkin method [2], boundary element-free method, RBF collocation methods (Kansa's methods) [17, 24], point interpolation (PI) method [30], DQ methods [14, 41], and so forth. They offer more advantages over mesh-dependent methods in treating the space-fractional PDEs but seldom works have been reported. Liu et. al proposed a PI method for the space-fractional diffusion equation [31]. Cheng et. al analysed an improved moving least-squares approximation to the solution of two-dimensional space-fractional wave equation [10]. Pang et. al extended DQ method to solve the space-fractional diffusion equation and use the as Lagrange interpolating basis functions as trial functions to determine the weighted coefficients [36].

DQ method is a kind of meshless methods which uses the weighted sum of functional values at sampling points along ordinate directions to discretize derivatives [3]. Subsequently, this kind of method enjoys the advantages as high accuracy, truly mesh-free, and the adaptability to high-dimensional problems. Regarding this point, in this article, we showcase an efficient RBFs-based DQ method for the following multi-term TSFDE on general domains:

(I) two-dimensional multi-term TSFDE:

$$\left\{ \begin{array}{l} P_{\theta_1, \theta_2, \dots, \theta_s} ({}_0^C D_t) u(x, y, t) - \varepsilon_\alpha^+(x, y) \frac{\partial_+^\alpha u(x, y, t)}{\partial x_+^\alpha} - \varepsilon_\alpha^-(x, y) \frac{\partial_-^\alpha u(x, y, t)}{\partial x_-^\alpha} \\ - \varepsilon_\beta^+(x, y) \frac{\partial_+^\beta u(x, y, t)}{\partial y_+^\beta} - \varepsilon_\beta^-(x, y) \frac{\partial_-^\beta u(x, y, t)}{\partial y_-^\beta} = f(x, y, t), \quad (x, y; t) \in \Omega \times (0, T], \\ u(x, y, 0) = u_0(x, y), \quad (x, y) \in \Omega, \\ u(x, y, t) = g(x, y, t), \quad (x, y; t) \in \partial\Omega \times (0, T], \end{array} \right. \quad (1.1)$$

where $0 < \theta_1, \theta_2, \dots, \theta_s < 1$, $s \in \mathbb{N}$, $1 < \alpha, \beta < 2$, $\Omega \subset \mathbb{R}^2$ with $\partial\Omega$ being its boundary, $\varepsilon_\zeta^\pm(x, y)$ are the diffusion coefficients with $\zeta = \alpha, \beta$.

(II) three-dimensional multi-term TSFDE:

$$\left\{ \begin{array}{l} P_{\theta_1, \theta_2, \dots, \theta_s} ({}_0^C D_t) u(x, y, z, t) - \varepsilon_\alpha^+(x, y, z) \frac{\partial_+^\alpha u(x, y, z, t)}{\partial x_+^\alpha} - \varepsilon_\alpha^-(x, y, z) \frac{\partial_-^\alpha u(x, y, z, t)}{\partial x_-^\alpha} - \varepsilon_\beta^+(x, y, z) \frac{\partial_+^\beta u(x, y, z, t)}{\partial y_+^\beta} \\ - \varepsilon_\beta^-(x, y, z) \frac{\partial_-^\beta u(x, y, z, t)}{\partial y_-^\beta} - \varepsilon_\gamma^+(x, y, z) \frac{\partial_+^\gamma u(x, y, z, t)}{\partial z_+^\gamma} + \varepsilon_\gamma^-(x, y, z) \frac{\partial_-^\gamma u(x, y, z, t)}{\partial z_-^\gamma} = f(x, y, z, t), \quad (x, y, z; t) \in \Omega \times (0, T], \\ u(x, y, z, 0) = u_0(x, y, z), \quad (x, y, z) \in \Omega, \\ u(x, y, z, t) = g(x, y, z, t), \quad (x, y, z; t) \in \partial\Omega \times (0, T], \end{array} \right. \quad (1.2)$$

where $0 < \theta_1, \theta_2, \dots, \theta_s < 1$, $s \in \mathbb{N}$, $1 < \alpha, \beta, \gamma < 2$, $\Omega \subset \mathbb{R}^3$ with $\partial\Omega$ being its boundary, $\varepsilon_\zeta^\pm(x, y, z)$ are the diffusion coefficients with $\zeta = \alpha, \beta, \gamma$.

The fractional derivatives in Eqs. (1.1)-(1.2) are defined in Caputo sense. More precisely, the ones tagged with "+" are the left-side derivatives, while those tagged with "-" are the right-side derivatives. For example, assuming $C_1 : x = x_L(y, z)$, $C_2 : x = x_R(y, z)$ the left and right boundaries of $\Omega \subset \mathbb{R}^3$, in which,

$$\begin{aligned} x_L(y, z) &= \min\{x : (x, \eta, \zeta), \eta = y, \zeta = z\}, \\ x_R(y, z) &= \max\{x : (x, \eta, \zeta), \eta = y, \zeta = z\}, \end{aligned}$$

then $\frac{\partial_+^\alpha u(x,y,z,t)}{\partial x_+^\alpha}$, $\frac{\partial_-^\alpha u(x,y,z,t)}{\partial x_-^\alpha}$ are defined as follows:

$$\frac{\partial_+^\alpha u(x,y,z,t)}{\partial x_+^\alpha} = \frac{1}{\Gamma(2-\alpha)} \int_{x_L(y,z)}^x \frac{\partial^2 u(\xi,y,z,t)}{\partial \xi^2} \frac{d\xi}{(x-\xi)^{\alpha-1}},$$

$$\frac{\partial_-^\alpha u(x,y,z,t)}{\partial x_-^\alpha} = \frac{1}{\Gamma(2-\alpha)} \int_x^{x_R(y,z)} \frac{\partial^2 u(\xi,y,z,t)}{\partial \xi^2} \frac{d\xi}{(\xi-x)^{\alpha-1}},$$

with the Gamma function $\Gamma(\cdot)$.

The fractional derivatives in other coordinate directions can be defined in the same fashion. $P_{\theta_1, \theta_2, \dots, \theta_s}({}_0^C D_t)$ denotes the multi-term fractional derivative operator:

$$P_{\theta_1, \theta_2, \dots, \theta_s}({}_0^C D_t)u(x,y,z,t) = \sum_{r=1}^s a_r {}_0^C D_t^{\theta_r} u(x,y,z,t) \quad (1.3)$$

$$= a_1 {}_0^C D_t^{\theta_1} u(x,y,z,t) + a_2 {}_0^C D_t^{\theta_2} u(x,y,z,t) + \dots + a_s {}_0^C D_t^{\theta_s} u(x,y,z,t), \quad (1.4)$$

where

$${}_0^C D_t^{\theta_r} u(x,y,z,t) = \frac{1}{\Gamma(1-\theta_r)} \int_0^t \frac{\partial u(x,y,z,\xi)}{\partial \xi} \frac{d\xi}{(t-\xi)^{\theta_r}}.$$

The outline is as follows. In Section 2, some preliminaries on fractional calculus and RBFs are introduced. In Section 3 the DQ approximation of fractional derivative is proposed based on RBFs. In Section 4, using the RBFs-based DQ formulas, we construct a fully discrete DQ method for the multi-term TSFDE on general domains and its algorithm is further studied in Section 5. In Section 6, some numerical tests are presented to confirm its convergence. In the last section, a brief summary is drawn.

2. Preliminaries

We recall some basic preliminaries on fractional calculus and RBFs required for further discussions.

2.1. Fractional calculus

Definition 2.1. The left and right Riemann-Liouville fractional integrals of order α are defined by

$${}_a J_x^{(\alpha)} u(x) = \frac{1}{\Gamma(\alpha)} \int_a^x \frac{u(\xi) d\xi}{(x-\xi)^{1-\alpha}}, \quad x > a,$$

$${}_x J_b^{(\alpha)} u(x) = \frac{1}{\Gamma(\alpha)} \int_x^b \frac{u(\xi) d\xi}{(x-\xi)^{1-\alpha}}, \quad x < b,$$

and if $\alpha = 0$, ${}_a J_x^{(0)} u(x) = u(x)$ and ${}_x J_b^{(0)} u(x) = u(x)$.

Definition 2.2. The left and right Riemann-Liouville fractional derivatives of order α are defined by

$${}_a^{RL} D_x^\alpha u(x) = D^n {}_a J_x^{(n-\alpha)} u(x) = \frac{1}{\Gamma(n-\alpha)} \frac{\partial^n}{\partial x^n} \int_a^x \frac{u(\xi) d\xi}{(x-\xi)^{\alpha-n+1}}, \quad x > a,$$

$${}_x^{RL} D_b^\alpha u(x) = D^n {}_x J_b^{(n-\alpha)} u(x) = \frac{(-1)^n}{\Gamma(n-\alpha)} \frac{\partial^n}{\partial x^n} \int_x^b \frac{u(\xi) d\xi}{(x-\xi)^{\alpha-n+1}}, \quad x < b,$$

where $n-1 < \alpha < n$, $n \in \mathbb{Z}^+$, and if $\alpha = n$, ${}_a^{RL} D_x^n u(x) = u^{(n)}(x)$ and ${}_x^{RL} D_b^n u(x) = (-1)^n u^{(n)}(x)$.

Definition 2.3. The left and right Caputo fractional derivatives of order α are defined by

$${}_a^C D_x^\alpha u(x) = {}_a J_x^{(n-\alpha)} u^{(n)}(x) = \frac{1}{\Gamma(n-\alpha)} \int_a^x \frac{\partial^n u(\xi)}{\partial \xi^n} \frac{d\xi}{(x-\xi)^{\alpha-n+1}}, \quad x > a,$$

$${}_x^C D_b^\alpha u(x) = {}_x J_b^{(n-\alpha)} u^{(n)}(x) = \frac{(-1)^n}{\Gamma(n-\alpha)} \int_x^b \frac{\partial^n u(\xi)}{\partial \xi^n} \frac{d\xi}{(x-\xi)^{\alpha-n+1}}, \quad x < b,$$

where $n-1 < \alpha < n$, $n \in \mathbb{Z}^+$, and if $\alpha = n$, ${}_a^C D_x^n u(x) = u^{(n)}(x)$ and ${}_x^C D_b^n u(x) = (-1)^n u^{(n)}(x)$.

The two frequently-used fractional derivatives are equivalent with exactness to an additive factor:

$${}_a^C D_x^\alpha u(x) = {}_a^{RL} D_x^\alpha u(x) - \sum_{l=0}^{n-1} \frac{u^{(l)}(a)(x-a)^{l-\alpha}}{\Gamma(l+1-\alpha)}, \quad (2.5)$$

$${}_x^C D_b^\alpha u(x) = {}_x^{RL} D_b^\alpha f(x) - \sum_{l=0}^{n-1} \frac{u^{(l)}(b)(b-x)^{l-\alpha}}{\Gamma(l+1-\alpha)}. \quad (2.6)$$

Moreover, we easily realize the following properties:

$${}_a^C D_x^\alpha C = 0, \quad (2.7)$$

$${}_a J_x^{(\alpha_1)} {}_a J_x^{(\alpha_2)} u(x) = {}_a J_x^{(\alpha_2)} {}_a J_x^{(\alpha_1)} u(x) = {}_a J_x^{(\alpha_1+\alpha_2)} u(x), \quad (2.8)$$

$${}_a^C D_x^\alpha (x-a)^\beta = {}_a^{RL} D_x^\alpha (x-a)^\beta = \frac{\Gamma(1+\beta)(x-a)^{\beta-\alpha}}{\Gamma(1+\beta-\alpha)}, \quad (2.9)$$

where C is a constant and $l > [\alpha] + 1$ with $[x]$ being the ceiling function, which outputs the smallest integer greater than or equal to x . Another point need to be noticed is that these properties are also true for the right-side fractional calculus. For more details, we refer the readers to [25] for overview.

2.2. Radial basis functions

Letting $\mathbf{x} = (x_1, x_2, \dots, x_d)$, $\{\mathbf{x}_k\}_{k=0}^{M_b} \in \Omega \subset \mathbb{R}^d$ and $\|\cdot\|$ be Euclidean norm, the approximation of $u(x)$ can be written as a weighted sum of RBFs in the form:

$$u(\mathbf{x}) \approx \sum_{k=0}^{M_b} \lambda_k \varphi_k(\mathbf{x}) + \sum_{l=1}^{M_p} \mu_l p_l(\mathbf{x}), \quad \mathbf{x} \in \Omega, \quad (2.10)$$

where $d = 1, 2, 3$, $M_p = (r+d-1)!/(d!(r-1)!)$, $\{\lambda_k\}_{k=0}^{M_b}$, $\{\mu_l\}_{l=1}^{M_p}$ are unknown weights, $\{\mu_l(\mathbf{x})\}_{l=1}^{M_p}$ are the basis functions of the polynomial space of degree at most $r-1$, and $\{\varphi_k(\mathbf{x})\}_{k=1}^{M_p}$ are RBFs, which defined by $\varphi_k(\mathbf{x}) = \varphi(\|\mathbf{x} - \mathbf{x}_k\|)$. To ensure that the interpolant properly behave at infinity, the above equations are augmented by

$$\sum_{l=0}^{M_p} \mu_l(t) p_l(\mathbf{x}_k) = 0, \quad l = 1, 2, \dots, M_p. \quad (2.11)$$

Putting Eqs. (2.10)-(2.11) in matrix form leads to a matrix system:

$$\begin{bmatrix} \mathbf{A} & \mathbf{B}^T \\ \mathbf{B} & \mathbf{0} \end{bmatrix} \begin{Bmatrix} \lambda \\ \mu \end{Bmatrix} = \begin{Bmatrix} \mathbf{u} \\ \mathbf{0} \end{Bmatrix}, \quad (2.12)$$

where the matrix elements for $[\mathbf{A}]$ are $\varphi_j(\mathbf{x}_i)$ and for $[\mathbf{B}]$ are $p_j(\mathbf{x}_i)$.

The RBFs provides an effective tool for the interpolation of scattered data in multi-dimensional domains. Since they only take the space distance as independent variable, as compared to the traditional basis function defined along coordinates, RBFs have the advantages of concise form, dimension-independent and isotropic properties. In particular, in the application of solving high-dimensional PDEs, the RBFs interpolation shows great flexibility. The numerical methods constructed by RBFs not only have the simplicity in the implementation, but also avoid the tedious mesh generation, and thereby reducing the pre-processing process of algorithms. If $r = \|\mathbf{x} - \mathbf{x}_k\|$, then the commonly used RBFs are listed in Table 1.

Definition 2.4. A function is completely monotonic if and only if $(-1)^\ell f^{(\ell)}(r) \geq 0$, for $\ell = 0, 1, 2, \dots$, and $r \geq 0$.

Theorem 2.1. [9] Let an univariate function $\psi(r) \in C^\infty[0, +\infty)$ be such that ψ is completely monotonic, but not a constant. Suppose further that $\psi(0) \geq 0$. Then the interpolation matrix $[\mathbf{A}]$ of the basis function $\psi(r^2)$ is positive definite.

Table 1: Some commonly used RBFs.

Name	RBF
Multiquadric (MQ)	$(r^2 + c^2)^{1/2}, c > 0$
Reciprocal Multiquadric (RMQ)	$1/(r^2 + c^2)^{1/2}, c > 0$
Inverse Quadratic (IQ)	$1/(r^2 + c^2), c > 0$
Polyharmonic Spline (PS)	$(-1)^{k+1} r^{2k} \ln r, k \in \mathbb{Z}^+$
Gaussian (GA)	$e^{-r^2/c^2}, c > 0$

The Eq. (2.12) is solved for $\{\lambda_k\}_{k=0}^{M_b}$, $\{\mu_l\}_{l=1}^{M_p}$ and the interpolation matrix $[\mathbf{A}]$ should be positive definite so that it invertible. According to Theorem 4.1, Reciprocal Multiquadratics, Inverse Quadratics and Gaussians are positive definite while Multiquadratics are only conditionally positive definite. Therefore, the polynomial term on the right-side of Eq. 2.10 can be removed for Reciprocal Multiquadratics, Inverse Quadratics and Gaussians while it is indispensable to Multiquadratics to maintain the well-posedness of the resulting algebraic system.

3. The DQ approximation of fractional derivative

In this section, we derive a new class of DQ formulas for fractional derivatives by RBFs as the trial functions. The DQ formula employs the linear sum of function values at discrete points to approximate partial derivatives with regard to an independent variable. Supposing $u(\mathbf{x}) \in C^k(\Omega)$, $k \in \mathbb{Z}^+$, we have the following DQ formula [41]:

$$u_x^{(m)}(\mathbf{x}_i, t) \approx \sum_{j=0}^M w_{ij}^m u(\mathbf{x}_j, t), \quad i, k = 0, 1, \dots, M, \quad (3.13)$$

where w_{ij}^m , $i, j = 1, 2, \dots, M$, are weighted coefficients. By realizing the essence of DQ formula, we propose the following DQ approximations to the left-hand fractional derivatives:

$$\frac{\partial_+^\alpha u(\mathbf{x}_i, t)}{\partial x_+^\alpha} \approx \sum_{j=0}^M w_{ij}^{\alpha^+} u(\mathbf{x}_j, t), \quad i, k = 0, 1, \dots, M, \quad (3.14)$$

where $w_{ij}^{\alpha^+}$, $w_{ij}^{\beta^+}$, $w_{ij}^{\gamma^+}$, $i, j = 1, 2, \dots, M$, are the related weighted coefficients, which satisfy

$$\frac{\partial_+^\alpha \phi_k(\mathbf{x}_i)}{\partial x_+^\alpha} = \sum_{j=0}^M w_{ij}^{\alpha^+} \phi_k(\mathbf{x}_j), \quad i, k = 0, 1, \dots, M, \quad (3.15)$$

with $\{\phi_k(\mathbf{x})\}_{k=0}^M$ being the trial functions. The weighted coefficients are determined by reforming Eqs. (3.15) in matrix system in advance. Likewise, we can extend the above formulas to the right-side fractional derivatives with regard to the variables x , y and z .

The calculation of weighted coefficients comprise a major part of DQ methods. In what follows, we show how to use the aforementioned RBFs to determine these coefficients. It should be noted that for Reciprocal Multiquadratics, Inverse Quadratics and Gaussians, their interpolation matrices invertible. Therefore, ignoring the polynomial terms on the right-side of RBFs interpolation (2.10) and substitute $\phi_k(\mathbf{x}_i) = \varphi_k(\mathbf{x}_i)$ into Eq. (3.15), we obtain the weighted coefficients by solving the resulting algebraic systems for each nodal point \mathbf{x}_i . As for Multiquadratics, we prefer to

$$u(\mathbf{x}, t) \approx \sum_{k=0}^M \lambda_k(t) \varphi_k(\mathbf{x}) + \mu_1(t). \quad (3.16)$$

To make the problem be well posed, one more equation is required. From Eq. (2.11), it follows that $\mu_1(t) = \sum_{k=0}^M \lambda_k(t)$, which further yields

$$u(\mathbf{x}, t) \approx \sum_{k=1}^M \lambda_k(t) \{\varphi_k(\mathbf{x}) - \varphi_0(\mathbf{x})\} + \mu_1(t).$$

By careful observation, we can consider $\phi_1(\mathbf{x}) = 1$, $\phi_i(\mathbf{x}) = \varphi_k(\mathbf{x}) - \varphi_0(\mathbf{x})$, $i = 1, 2, \dots, M$, as the trial functions. Referring to the above discussion and ${}_a^C D_x^\theta 1 = 0$, we obtain the algebraic system as follows

$$\mathbf{M} \mathbf{w}_i^{\alpha^+} = \mathbf{R}_i, \quad i = 1, 2, \dots, M, \quad (3.17)$$

where

$$\mathbf{M} = \begin{pmatrix} 1 & 1 & \cdots & 1 \\ \varphi_1(\mathbf{x}_0) - \varphi_0(\mathbf{x}_0) & \varphi_1(\mathbf{x}_1) - \varphi_0(\mathbf{x}_1) & \cdots & \varphi_1(\mathbf{x}_M) - \varphi_0(\mathbf{x}_M) \\ \vdots & \vdots & & \vdots \\ \varphi_M(\mathbf{x}_0) - \varphi_0(\mathbf{x}_0) & \varphi_M(\mathbf{x}_1) - \varphi_0(\mathbf{x}_1) & \cdots & \varphi_M(\mathbf{x}_M) - \varphi_0(\mathbf{x}_M) \end{pmatrix}, \quad \mathbf{w}_i^{\alpha^+} = \begin{pmatrix} w_{i0}^{\alpha^+} \\ w_{i1}^{\alpha^+} \\ \vdots \\ w_{iM}^{\alpha^+} \end{pmatrix}, \quad \mathbf{R}_i = \begin{pmatrix} 0 \\ \frac{\partial_x^\alpha \varphi_1(\mathbf{x}_i)}{\partial x_+^\alpha} - \frac{\partial_x^\alpha \varphi_0(\mathbf{x}_i)}{\partial x_+^\alpha} \\ \vdots \\ \frac{\partial_x^\alpha \varphi_M(\mathbf{x}_i)}{\partial x_+^\alpha} - \frac{\partial_x^\alpha \varphi_0(\mathbf{x}_i)}{\partial x_+^\alpha} \end{pmatrix}.$$

For each node \mathbf{x}_i , the values of unknown weighted coefficients are consequently computed by $\mathbf{w}_i^{\alpha^+} = \mathbf{M}^{-1} \mathbf{R}_i$.

We note that the DQ approximation (3.14) works because the fractional derivatives are linear operators. In other words, if $u(\mathbf{x}, t) \approx \sum_{k=0}^M \delta_k(t) \phi_k(\mathbf{x})$, $\mathbf{x} \in \Omega$, and the weighted coefficients fulfill Eqs. (3.15), then for $\frac{\partial_x^\alpha u(\mathbf{x}, t)}{\partial x_+^\alpha}$, we realize

$$\frac{\partial_x^\alpha u(\mathbf{x}_i, t)}{\partial x_+^\alpha} \approx \sum_{k=0}^M \delta_k(t) \frac{\partial_x^\alpha \phi_k(\mathbf{x}_i)}{\partial x_+^\alpha} = \sum_{k=0}^M \delta_k(t) \sum_{j=0}^M w_{ij}^{\alpha^+} \phi_k(\mathbf{x}_j) \approx \sum_{j=0}^M w_{ij}^{\alpha^+} u(\mathbf{x}_j, t) \quad (3.18)$$

through the linear property of fractional derivatives. In addition, it is sure that the above convergent result is exactly true for the right-side fractional derivatives with regard to the others variables.

4. The description of RBFs-based DQ method

4.1. Discretization of time-fractional derivative

In this subsection, we introduce high-order schemes to discretize the fractional derivative in temporal direction. To this end, we define a time lattice $t_n = n\tau$, $n = 0, 1, \dots, N$, $T = \tau N$, $N \in \mathbb{Z}^+$, and review the relationship between Caputo and Riemann-Liouville derivatives:

$${}_0^C D_t^\theta u(\mathbf{x}, t) = {}_0^{RL} D_t^\theta u(\mathbf{x}, t) - \sum_{l=0}^{m-1} \frac{u_t^{(l)}(\mathbf{x}, 0) t^{l-\theta}}{\Gamma(l+1-\theta)}, \quad (4.19)$$

where $m-1 < \theta < m$, $m \in \mathbb{Z}^+$. Using the property (2.9), we obtain a class of high-order schemes for Caputo derivative by applying the weighted and shifted Lubich difference operators $\mathcal{L}_q^\theta u(\mathbf{x}, t_n) = \frac{1}{\tau^\theta} \sum_{k=0}^n \omega_k^{q,\theta} u(\mathbf{x}, t_{n-k})$, $q = 1, 2, 3, 4, 5$, to discretize Riemann-Liouville derivatives on the right-side of Eq. (4.19), which reads

$${}_0^C D_t^\theta u(\mathbf{x}, t_n) \approx \frac{1}{\tau^\theta} \sum_{k=0}^n \omega_k^{q,\theta} u(\mathbf{x}, t_{n-k}) - \frac{1}{\tau^\theta} \sum_{l=0}^{m-1} \sum_{k=0}^n \frac{\omega_k^{q,\theta} u_t^{(l)}(\mathbf{x}, 0) t_{n-k}^l}{l!}, \quad (4.20)$$

where $\{\omega_k^{q,\theta}\}_{k=0}^n$ are the discrete coefficients [8]. For instance, if $q = 1$, we have $\omega_k^{1,\theta} = (-1)^k \binom{\theta}{k} = \frac{\Gamma(k-\theta)}{\Gamma(-\theta)\Gamma(k+1)}$, $k \geq 0$, and if $q = 3$, we have

$$\omega_k^{3,\theta} = \left(\frac{11}{6}\right)^\theta \sum_{p=0}^k \sum_{q=0}^p \mu^q \bar{\mu}^{p-q} \omega_q^{1,\theta} \omega_{p-q}^{1,\theta} \omega_{k-p}^{1,\theta}, \quad (4.21)$$

where $\mu = \frac{4}{7+\sqrt{39}i}$, $\bar{\mu} = \frac{4}{7-\sqrt{39}i}$, and i denotes imaginary unit.

Lemma 4.1. *The coefficients $\omega_k^{1,\theta}$ satisfy the following properties*

$$(i) \quad \omega_0^{1,\theta} = 1, \quad \omega_k^{1,\theta} < 0, \quad \sum_{k=0}^\infty \omega_k^{1,\theta} = 0, \quad \sum_{k=0}^{n-1} \omega_k^{1,\theta} > 0, \quad \forall k \geq 1,$$

$$(ii) \quad \omega_0^{1,\theta} = 1, \quad \omega_k^{1,\theta} = \left(1 - \frac{\theta+1}{k}\right) \omega_{k-1}^{1,\theta}, \quad \forall k \geq 1.$$

Lemma 4.2. [8] Assume that $u(\mathbf{x}, t)$, ${}_0^{RL}D_t^\theta u(\mathbf{x}, t)$ with $\theta > 0$ and their Fourier transforms belong to $L^1(\mathbb{R})$ with regard to t , then the Lubich difference operators satisfy

$${}_0^{RL}D_t^\theta u(\mathbf{x}, t) = \mathcal{L}_q^\theta u(\mathbf{x}, t) + \mathcal{O}(\tau^q). \quad (4.22)$$

Theorem 4.1. Assume that $u(\mathbf{x}, t)$, ${}_0^{RL}D_t^\theta u(\mathbf{x}, t)$ with $\theta > 0$ are smooth enough with regard to t , the we have

$${}_0^C D_t^\theta u(\mathbf{x}, t_n) = \mathcal{A}_q^\theta u(\mathbf{x}, t_n) + \mathcal{O}(\tau^q), \quad (4.23)$$

where

$$\mathcal{A}_q^\theta u(\mathbf{x}, t_n) = \frac{1}{\tau^\theta} \sum_{k=0}^n \omega_k^{q,\theta} u(\mathbf{x}, t_{n-k}) - \frac{1}{\tau^\theta} \sum_{l=0}^{m-1} \sum_{k=0}^n \frac{\omega_k^{q,\theta} u_t^{(l)}(\mathbf{x}, 0) t_{n-k}^l}{l!}.$$

Proof. The proof is trivial by following Lemma 4.2 and references [8, 12]. \square

Applying the operator \mathcal{A}_q^θ to the multi-term fractional derivative operator and set $0 < \theta < 1$, we finally obtain

$$\begin{aligned} P_{\theta_1, \theta_2, \dots, \theta_s} ({}_0^C D_t) u(\mathbf{x}, t_n) &= a_{10} {}_0^C D_t^{\theta_1} u(\mathbf{x}, t_n) + a_{20} {}_0^C D_t^{\theta_2} u(\mathbf{x}, t_n) + \dots + a_{s0} {}_0^C D_t^{\theta_s} u(\mathbf{x}, t_n) \\ &= a_1 \mathcal{A}_q^{\theta_1} u(\mathbf{x}, t_n) + a_2 \mathcal{A}_q^{\theta_2} u(\mathbf{x}, t_n) + \dots + a_s \mathcal{A}_q^{\theta_s} u(\mathbf{x}, t_n) + \mathcal{O}(\tau^q) \\ &= \sum_{r=1}^s a_r \mathcal{A}_q^{\theta_r} u(\mathbf{x}, t_n) + \mathcal{O}(\tau^q) \\ &= \sum_{r=1}^s \frac{a_r}{\tau^{\theta_r}} \sum_{k=0}^{n-1} \omega_k^{q,\theta_r} u(\mathbf{x}, t_{n-k}) - \sum_{r=1}^s \frac{a_r}{\tau^{\theta_r}} \sum_{k=0}^{n-1} \omega_k^{q,\theta_r} u(\mathbf{x}, 0) + \mathcal{O}(\tau^q). \end{aligned} \quad (4.24)$$

4.2. Fully discrete RBFs-based DQ scheme

In this subsection, we develop a fully discrete DQ scheme for the multi-term TSFDE, which utilizes the operator \mathcal{A}_q^θ to treat the Caputo derivative in time and RBFs-based DQ approximations for the fractional derivatives in space. For the ease of expression, letting $\mathbf{x} = (x_1, x_2, \dots, x_d)$, $\Omega \subset \mathbb{R}^d$, we put Eqs. (1.1)-(1.2) in the unified form:

$$\begin{cases} P_{\theta_1, \theta_2, \dots, \theta_s} ({}_0^C D_t) u(\mathbf{x}, t) - \sum_{l=1}^d \varepsilon_{\alpha_l}^+(\mathbf{x}) \frac{\partial^{\alpha_l} u(\mathbf{x}, t)}{\partial x_{l,+}^{\alpha_l}} - \sum_{l=1}^d \varepsilon_{\alpha_l}^-(\mathbf{x}) \frac{\partial^{\alpha_l} u(\mathbf{x}, t)}{\partial x_{l,-}^{\alpha_l}} = f(\mathbf{x}, t), & (\mathbf{x}; t) \in \Omega \times (0, T], \\ u(\mathbf{x}, 0) = u_0(\mathbf{x}), & \mathbf{x} \in \Omega, \\ u(\mathbf{x}, t) = g(\mathbf{x}, t), & (\mathbf{x}; t) \in \partial\Omega \times (0, T], \end{cases} \quad (4.25)$$

where $0 < \theta_1, \theta_2, \dots, \theta_s < 1$, $1 < \alpha_l < 2$ and $l = 1, 2, \dots, d$.

Let $\{\mathbf{x}_i\}_{i=0}^M$ be a set of nodes in $\Omega \subset \mathbb{R}^d$. Replacing the space-fractional derivatives by RBFs-based DQ formulas, we obtain the following multi-term fractional ODEs:

$$P_{\theta_1, \theta_2, \dots, \theta_s} ({}_0^C D_t) u(\mathbf{x}_i, t) - \sum_{l=1}^d \varepsilon_{\alpha_l}^+(\mathbf{x}_i) \sum_{j=0}^M w_{ij}^{\alpha_l^+} u(\mathbf{x}_j, t) - \sum_{l=1}^d \varepsilon_{\alpha_l}^-(\mathbf{x}_i) \sum_{j=0}^M w_{ij}^{\alpha_l^-} u(\mathbf{x}_j, t) = f(\mathbf{x}_i, t), \quad (4.26)$$

where $i = 1, 2, \dots, M$. Furthermore, using the operator \mathcal{A}_q^θ to discretize $P_{\theta_1, \theta_2, \dots, \theta_s} ({}_0^C D_t)$ arrives at

$$\sum_{r=1}^s a_r \mathcal{A}_q^{\theta_r} u(\mathbf{x}_i, t_n) - \sum_{l=1}^d \varepsilon_{\alpha_l}^+(\mathbf{x}_i) \sum_{j=0}^M w_{ij}^{\alpha_l^+} u(\mathbf{x}_j, t_n) - \sum_{l=1}^d \varepsilon_{\alpha_l}^-(\mathbf{x}_i) \sum_{j=0}^M w_{ij}^{\alpha_l^-} u(\mathbf{x}_j, t_n) = f(\mathbf{x}_i, t_n) + \mathcal{O}(\tau^q). \quad (4.27)$$

Ignoring $\mathcal{O}(\tau^q)$ and enforcing Eq. (4.27) exactly holds at $\{\mathbf{x}_i\}_{i=0}^M$, we obtain the fully discrete DQ scheme:

$$\begin{cases} \sum_{r=1}^s \frac{a_r \omega_0^{q,\theta_r}}{\tau^{\theta_r}} u(\mathbf{x}_i, t_n) - \sum_{l=1}^d \varepsilon_{\alpha_l}^+(\mathbf{x}_i) \sum_{j=0}^M w_{ij}^{\alpha_l^+} u(\mathbf{x}_j, t_n) - \sum_{l=1}^d \varepsilon_{\alpha_l}^-(\mathbf{x}_i) \sum_{j=0}^M w_{ij}^{\alpha_l^-} u(\mathbf{x}_j, t_n) \\ = f(\mathbf{x}_i, t_n) - \sum_{i=1}^s \frac{a_i}{\tau^{\theta_i}} \sum_{k=0}^{n-1} \omega_k^{q,\theta_i} u(\mathbf{x}_i, t_{n-k}) + \sum_{i=1}^s \frac{a_i}{\tau^{\theta_i}} \sum_{k=1}^{n-1} \omega_k^{q,\theta_i} u(\mathbf{x}_i, 0), & (\mathbf{x}_i; t_n) \in \Omega \times (0, T], \\ u(\mathbf{x}_i, 0) = u_0(\mathbf{x}_i), & \mathbf{x}_i \in \Omega, \\ u(\mathbf{x}_i, t_n) = g(\mathbf{x}_i, t_n), & (\mathbf{x}_i; t_n) \in \partial\Omega \times (0, T], \end{cases} \quad (4.28)$$

where $i = 1, 2, \dots, M$ and $n = 0, 1, \dots, N$.

In the sequel, we employ the notations $U_i^n = u(\mathbf{x}_i, t_n)$, $\varepsilon_{\alpha_l, i}^\pm = \varepsilon_{\alpha_l}^\pm(\mathbf{x}_i)$, $f_i^n = f(\mathbf{x}_i, t_n)$, $g_i^n = g(\mathbf{x}_i, t_n)$, and \mathbf{U}^n , \mathbf{F}^n , \mathbf{g}^n are the column vectors consisting of U_i^n , f_i^n , g_i^n in the ascending order of subscript i , respectively. Also, we adopt $\boldsymbol{\varepsilon}_{\alpha_l}^\pm = \text{diag}(\varepsilon_{\alpha_l, 0}^\pm, \varepsilon_{\alpha_l, 1}^\pm, \dots, \varepsilon_{\alpha_l, M}^\pm)$. Then, reforming Eqs. (4.28) in a matrix system leads to

$$\begin{cases} \sum_{r=1}^s \frac{a_r \omega_0^{q, \theta_r}}{\tau^{\theta_r}} \mathbf{U}^n - \sum_{l=1}^d \boldsymbol{\varepsilon}_{\alpha_l}^+ \mathbf{W}_{\alpha_l}^+ \mathbf{U}^n - \sum_{l=1}^d \boldsymbol{\varepsilon}_{\alpha_l}^- \mathbf{W}_{\alpha_l}^- \mathbf{U}^n \\ = \mathbf{F}^n - \sum_{r=1}^s \frac{a_r}{\tau^{\theta_r}} \sum_{k=0}^{n-1} \omega_k^{q, \theta_r} \mathbf{U}^{n-k} + \sum_{r=1}^s \frac{a_r}{\tau^{\theta_r}} \sum_{k=1}^{n-1} \omega_k^{q, \theta_r} \mathbf{U}^0, \\ \mathbf{U}^n = \mathbf{g}^n, \quad n = 0, 1, \dots, N, \end{cases} \quad (4.29)$$

where $\mathbf{W}_{\alpha_l}^\pm$ are the weighted coefficient matrices, given by

$$\mathbf{W}_{\alpha_l}^\pm = \begin{pmatrix} w_{00}^{\alpha_l^\pm} & w_{01}^{\alpha_l^\pm} & \cdots & w_{0,M}^{\alpha_l^\pm} \\ w_{10}^{\alpha_l^\pm} & w_{11}^{\alpha_l^\pm} & \cdots & w_{1,M}^{\alpha_l^\pm} \\ \vdots & \vdots & \ddots & \vdots \\ w_{M,0}^{\alpha_l^\pm} & w_{M,1}^{\alpha_l^\pm} & \cdots & w_{M,M}^{\alpha_l^\pm} \end{pmatrix}, \quad l = 1, 2, \dots, d.$$

Handling the boundary conditions properly and solving the algebraic equations resulting from the scheme (4.29) at each time step, we thus obtain the desirable solutions for the considered problem on all time layers.

5. Algorithm and implementation

In this section, we turn our eyes to the implementation of the proposed scheme (4.29). To perform the algorithm, an important problem having to be addressed is how to compute the fractional derivatives of RBFs and determine the corresponding integral paths. It is acknowledged that the fractional derivative of a general function as RBFs is difficult to compute. Hereafter, we will be engaged in this point. For a node $\mathbf{x}_k \in \Omega$ and the RBF $\varphi_k(\mathbf{x})$, letting $\xi = x_l - (x_l - X_{l,L})(1 + \zeta)/2$, one has

$$\frac{\partial_\zeta^\alpha \varphi_k(x_1, x_2, \dots, x_d)}{\partial x_{l,+}^\alpha} = \frac{1}{\Gamma(2 - \alpha)} \left(\frac{x_l - X_{l,L}}{2} \right)^{2-\alpha} \int_{-1}^1 (1 + \zeta)^{1-\alpha} \frac{\partial^2 \varphi_k(\dots, x_l - (x_l - X_{l,L})(1 + \zeta)/2, \dots)}{\partial x_l^2} d\zeta, \quad (5.30)$$

where $X_{l,L} = \min \{\eta_l : (\eta_1, \eta_2, \dots, \eta_d), \eta_i = x_i, i \neq l\}$. Then, it can be treated by Gauss-Jacobi quadrature formula [35]. The line segment along the x_l -coordinate axis from the left-side of boundary to the node x_l is called the integral path, which need to be determined before the calculation of fractional derivatives.

Hereafter, we will carefully illustrate how to perform the RBFs-based DQ scheme. Using Matlab as a platform for programming, some common commands in Matlab will be used as symbols. Let nonb , boup be the index vectors of the internal and boundary nodes of Ω , respectively. For the sake of simplicity, we define $\mathbf{U}^n(\text{nonb})$, $\mathbf{I} = \text{eye}(\text{length}(\text{boup}))$, $\tilde{\boldsymbol{\varepsilon}}_l^\pm = \boldsymbol{\varepsilon}_{\alpha_l}^\pm(\text{nonb}, \text{nonb})$, $\mathbf{K}_{\alpha_l}^\pm = \mathbf{W}_{\alpha_l}^\pm(\text{nonb}, \text{nonb})$, $\mathbf{G}_{\alpha_l}^\pm = \mathbf{W}_{\alpha_l}^\pm(\text{nonb}, \text{boup})$, $\tilde{\mathbf{F}}^n = \mathbf{F}^n(\text{nonb})$ and $\tilde{\mathbf{g}}^n = \mathbf{g}^n(\text{nonb})$. Imposing the boundary condition, we obtain the following RBFs-based DQ scheme

$$\begin{aligned} & \left(\sum_{r=1}^s \frac{a_r \omega_0^{q, \theta_r}}{\tau^{\theta_r}} \mathbf{I} - \sum_{l=1}^d \tilde{\boldsymbol{\varepsilon}}_l^+ \mathbf{K}_{\alpha_l}^+ - \sum_{l=1}^d \tilde{\boldsymbol{\varepsilon}}_l^- \mathbf{K}_{\alpha_l}^- \right) \tilde{\mathbf{U}}^n \\ &= \mathbf{P}^n - \sum_{r=1}^s \frac{a_r}{\tau^{\theta_r}} \sum_{k=1}^{n-1} \omega_k^{q, \theta_r} \tilde{\mathbf{U}}^{n-k} + \sum_{r=1}^s \frac{a_r}{\tau^{\theta_r}} \sum_{k=0}^{n-1} \omega_k^{q, \theta_r} \tilde{\mathbf{U}}^0, \end{aligned} \quad (5.31)$$

with the right-hand vector

$$\mathbf{P}^n = \tilde{\mathbf{F}}^n + \sum_{p=1}^Q \sum_{l=1}^L \tilde{\boldsymbol{\varepsilon}}_l^+ \tilde{\mathbf{g}}^n(p) \mathbf{G}_{\alpha_l}^+(:, p) + \sum_{p=1}^Q \sum_{l=1}^L \tilde{\boldsymbol{\varepsilon}}_l^- \tilde{\mathbf{g}}^n(p) \mathbf{G}_{\alpha_l}^-(:, p), \quad Q = \text{length}(\text{boup}), \quad (5.32)$$

which can be directly implemented, where $\mathbf{U}^n(nonb)$ are the unknown vectors which yet to be determined. A detailed implementation of the algorithm for the scheme (5.31)-(5.32) is presented in Algorithm 1.

Algorithm 1: Implementation of RBFs-based DQ algorithm

Assign α_l, θ_l, q and allocate $\{t_n\}_{n=0}^N, \{\mathbf{x}_i\}_{i=0}^M$.
Get internal and boundary nodes and their index vectors $nonb, boup$.
Define the matrices $\mathbf{U}, \mathbf{W}_{\alpha_l}^\pm$ and form $\mathbf{\tilde{e}}_l^\pm, \mathbf{M}$.
for $i \leq M$ **do**
 Determine the line segment along coordinate axis for \mathbf{x}_i .
 Compute the fractional derivatives of RBFs and get $\mathbf{W}_{\alpha_l}(i+1,:) = (\mathbf{w}_i^{\alpha_l^\pm})^T$.
end for
Compute $\mathbf{\tilde{e}}_l^\pm, \mathbf{K}_{\alpha_l}^\pm, \mathbf{G}_{\alpha_l}^\pm, \mathbf{F}^n, \mathbf{\tilde{g}}^n$ and $\mathbf{I} = eye(length(boup))$.
Generate the discrete coefficients $\omega_j^{q, \theta_l}, j = 0, 1, 2, \dots$
Define the matrix $\mathbf{K} = \left(\sum_{r=1}^s \frac{a_r \omega_r^{q, \theta_l}}{\tau_r^{\theta_l}} \mathbf{I} - \sum_{l=1}^d \mathbf{\tilde{e}}_l^+ \mathbf{K}_{\alpha_l}^+ - \sum_{l=1}^d \mathbf{\tilde{e}}_l^- \mathbf{K}_{\alpha_l}^- \right)$.
for $n \leq N$ **do**
 $\mathbf{P}^n = \sum_{r=1}^s \frac{a_r}{\tau_r^{\theta_l}} \omega_r^{q, \theta_l} \mathbf{\tilde{U}}^0$.
 for $k \leq n-1$ **do**
 $\mathbf{P}^n = \mathbf{P}^{n-1} - \sum_{r=1}^s \frac{a_r}{\tau_r^{\theta_l}} \omega_r^{q, \theta_l} \mathbf{U}(nonb, n-k+1) + \sum_{r=1}^s \frac{a_r}{\tau_r^{\theta_l}} \omega_r^{q, \theta_l} \mathbf{U}(nonb, 1)$.
 end for
 $\mathbf{R}^n = \mathbf{P}^n + \mathbf{\tilde{F}}^n$.
 for $p \leq Q$ **do**
 $\mathbf{R}^n = \mathbf{R}^n + \sum_{l=1}^L \mathbf{\tilde{e}}_l^+ \mathbf{\tilde{g}}^n(p) \mathbf{G}_{\alpha_l}^+(:, p) + \sum_{l=1}^L \mathbf{\tilde{e}}_l^- \mathbf{\tilde{g}}^n(p) \mathbf{G}_{\alpha_l}^-(:, p)$.
 end for
 Solve $\mathbf{\tilde{U}}^n = \mathbf{R}^n \setminus \mathbf{K}$ to obtain $\mathbf{\tilde{U}}^n$.
 Set $\mathbf{U}(nonb, n+1) = \mathbf{\tilde{U}}^n$ and $\mathbf{U}(boun, n+1) = \mathbf{\tilde{g}}^n$.
end for
Return \mathbf{U}

6. Numerical examples

Let u_j^n, U_j^n be the exact and numerical solutions at the time level n . Denoting

$$\|u - U\|_{L^2} = \left[h^* \sum_{j=0}^M (u_j^n - U_j^n)^2 \right]^{\frac{1}{2}}, \quad h^* = \frac{1}{M+1},$$

$$\|u - U\|_{L^\infty} = \max_{0 \leq j \leq M} |u_j^n - U_j^n|,$$

some illustrative examples will be performed to reveal the validity and efficiency of the proposed RBFs-based DQ method. In the runs, we choose the values of shape parameters with reference to the formula $c = \nu/(M+1)^{\sigma/4}$ or artificially choose their values, where $\nu > 0, \sigma \in \mathbb{Z}^+$. Besides, we solve all one-dimensional problems by using the nodal distribution $x_i = (1 - \cos \frac{i\pi}{M})(b-a)/2 + a, i = 0, 1, \dots, M$, when $\Omega = [a, b]$.

6.1. One-dimensional problems

Example 6.1. To test the validity of the DQ formula, we discretize the left-side fractional derivative ${}_{-1}^C D_x^\alpha (x+1)^3$ on $[-1, 1]$ by Grünwald-Letnikov (GL) difference operator and DQ formula, in which case, one has

$${}_{-1}^C D_x^\alpha (x+1)^3 = \frac{6(x+1)^{3-\alpha}}{\Gamma(4-\alpha)}.$$

We choose $\alpha = 1.5$ and Reciprocal Multiquadratics as the trial functions. The comparisons of numerical errors and convergent rates (*Cov.rate*) of these two methods are given in Table 2. It can be seen that the convergence rates of GL-operator is strictly 1, while the convergence rates of DQ formula is much higher than GL-operator, and the errors of DQ formula are less than GL-operator. Thus, our DQ formulas are effective and more efficient than GL-operator.

Table 2: The comparisons of GL-operator and DQ formula when $\alpha = 1.5$.

M	GL-operator		DQ formula, $\nu = 1.3$, $\sigma = 1$	
	$\ u - U\ _{L^2}$	Cov.rate	$\ u - U\ _{L^2}$	Cov.rate
10	3.1748e-01	-	5.4602e-01	-
15	2.1632e-01	0.95	8.7341e-02	4.52
20	1.6399e-01	0.96	2.3303e-02	4.59
25	1.3203e-01	0.97	6.8577e-03	5.48

Example 6.2. Consider the one-dimensional multi-term TSFDE:

$$\begin{cases} \sum_{r=1}^4 a_{r0} {}_0^C D_t^{\theta_r} u(x, t) - \frac{\partial_+^\alpha u(x, t)}{\partial x_+^\alpha} = \sum_{r=1}^4 \frac{120 a_r t^{5-\theta_r}}{\Gamma 6 - \theta_r} - \frac{24 t^5 x^{4-\alpha}}{\Gamma(5-\alpha)}, & (x, t) \in [0, 1] \times (0, T], \\ u(x, 0) = 0, \quad x \in [0, 1], \\ u(0, t) = 0, \quad u(1, t) = t^5, \quad t \in (0, T], \end{cases} \quad (6.33)$$

with $a_1 = a_2 = a_3 = a_4 = 1$, $\theta_1 = 0.3$, $\theta_2 = 0.5$, $\theta_3 = 0.7$, $\theta_4 = 0.9$ and $\alpha = 1.2$. The exact solution is given by $u(x, t) = t^5 x^4$. Using Multiquadratics and Inverse Quadratics as the trial functions, the numerical results in space at $t = 0.5$ with $q = 1$, $\tau = 5.0 \times 10^{-5}$ are listed in Table 3. Further, we test the convergent rates of the MQ-based DQ scheme in time with different q . For this purpose, taking $M = 50$ and $q = 1, 2, 3, 4$, the numerical errors and convergent rates at $t = 0.5$ are all presented in 4, which confirm the convergent accuracy $\mathcal{O}(\tau^q)$.

Table 3: The numerical results at $t = 0.5$ with $q = 1$ and $\alpha = 1.2$ for Example 6.2.

M	MQ-based DQ method, $\nu = 0.1$, $\sigma = 1$		IQ-based DQ method, $\nu = 0.3$, $\sigma = 1$	
	$\ u - U\ _{L^2}$	Cov.rate	$\ u - U\ _{L^2}$	Cov.rate
10	6.7983e-05	-	1.3132e-04	-
15	1.7258e-05	3.38	3.1071e-05	3.55
20	6.5139e-06	3.39	9.2979e-06	4.19
25	2.9562e-06	3.54	3.3970e-06	4.51

6.2. Two-dimensional problems

Example 6.3. Consider the two-dimensional multi-term TSFDE:

$$\begin{cases} {}_0^C D_t^\theta u(x, y, t) + \frac{1}{2 \cos(\alpha\pi/2)} \left(\frac{\partial_+^\alpha u(x, y, t)}{\partial x_+^\alpha} + \frac{\partial_-^\alpha u(x, y, t)}{\partial x_-^\alpha} \right) \\ \quad + \frac{1}{2 \cos(\beta\pi/2)} \left(\frac{\partial_+^\beta u(x, y, t)}{\partial y_+^\beta} + \frac{\partial_-^\beta u(x, y, t)}{\partial y_-^\beta} \right) = f(x, y, t), \quad (x, y, t) \in \Omega \times (0, T], \\ u(x, y, 0) = x^2(1-x)^2 y^2(1-y)^2, \quad (x, y) \in \Omega, \\ u(x, y, t) = 0, \quad (x, y, t) \in \partial\Omega \times (0, T], \end{cases} \quad (6.34)$$

Table 4: The numerical results at $t = 0.5$ of MQ-based DQ method with $\nu = 0.15$, $\sigma = 1$ and $\alpha = 1.2$ for Example 6.2.

	τ	$\ u - U\ _{L^2}$	Cov.rate	$\ u - U\ _{L^\infty}$	Cov.rate
$q = 1$	1/10	2.4414e-03	-	5.0450e-03	-
	1/20	1.2432e-03	0.97	2.6025e-03	0.96
	1/40	6.2677e-04	0.99	1.3202e-03	0.98
	1/80	3.1463e-04	0.99	6.6470e-04	0.99
$q = 2$	1/10	8.5486e-04	-	1.7887e-03	-
	1/20	2.5813e-04	1.73	5.4164e-04	1.72
	1/40	7.1272e-05	1.86	1.4945e-04	1.86
	1/80	1.8741e-05	1.93	3.9271e-05	1.93
$q = 3$	1/10	3.2489e-04	-	6.7717e-04	-
	1/20	5.2081e-05	2.64	1.0742e-04	2.66
	1/40	7.2778e-06	2.84	1.4941e-05	2.85
	1/80	9.6000e-07	2.92	1.9623e-06	2.93
$q = 4$	1/10	1.0892e-04	-	2.2404e-04	-
	1/20	7.8556e-06	3.79	1.5722e-05	3.83
	1/40	5.2432e-07	3.91	1.0391e-06	3.92
	1/80	3.9482e-08	3.73	1.1705e-07	3.15

with $\theta = 0.5$, $\alpha = \beta = 1.6$, $\Omega = [0, 1] \times [0, 1]$ and the source term

$$\begin{aligned}
 f(x, y, t) = & \frac{2t^{2-\alpha}}{\Gamma(3-\alpha)} x^2 (1-x)^2 y^2 (1-y)^2 \\
 & + \frac{(1+t^2)y^2(1-y)^2}{\cos(\beta\pi/2)} \left\{ \frac{x^{2-\beta} + (1-x)^{2-\beta}}{\Gamma(3-\beta)} - \frac{6(x^{2-\beta} + (1-x)^{2-\beta})}{\Gamma(4-\beta)} + \frac{12(x^{2-\beta} + (1-x)^{2-\beta})}{\Gamma(5-\beta)} \right\} \\
 & + \frac{(1+t^2)x^2(1-x)^2}{\cos(\beta\pi/2)} \left\{ \frac{y^{2-\beta} + (1-y)^{2-\beta}}{\Gamma(3-\beta)} - \frac{6(y^{2-\beta} + (1-y)^{2-\beta})}{\Gamma(4-\beta)} + \frac{12(y^{2-\beta} + (1-y)^{2-\beta})}{\Gamma(5-\beta)} \right\}.
 \end{aligned}$$

The exact solution is $u(x, y, t) = (1+t^2)x^2(1-x)^2y^2(1-y)^2$. To show the superiority of the method as much as possible, we compare the spatial accuracy of the weighted shifted GL methods (WSGL)[40] ($(p, q) = (1, 0)$ for WSGL1 and $(p, q) = (1, -1)$ for WSGL2), FD and FE methods [7, 37], and our DQ methods based on Reciprocal Multiquadratics in term of $\|u - U\|_{L^2}$. Taking $\tau = 1.0 \times 10^{-3}$, $\nu = 8$ and $\sigma = 2$, the numerical errors at $t = 1$ of all above methods are presented in Table 5. In Fig. ??, the used configuration of 289 nodes and its corresponding error distribution of RMQ-based DQ method are presented. We observe that our method is more accurate than WSGL and FD method by using the same discrete parameters. Although the error magnitude of DQ method is about the same as FE method, it is sure that our method is more flexible in implementation and has a less amount of computation.

 Table 5: The comparisons of GL, FD, FE and DQ methods at $t = 1$ when $\theta = 0.5$, $\alpha = \beta = 1.6$

M	WSGL1[40]	WSGL2[40]	FD method[7]	FE method[37]	RMQ-based DQ method
25	8.2885e-04	7.1069e-04	5.1926e-04	2.8397e-04	2.4378e-04
81	2.0070e-04	2.4232e-04	1.1762e-05	8.6729e-05	7.7419e-05
289	4.8865e-05	6.9518e-05	2.6904e-05	2.2360e-05	2.1523e-05
1089	1.1904e-05	1.8377e-05	6.2224e-06	5.1208e-06	6.5475e-06

Example 6.4. Consider the two-dimensional multi-term TSFDE:

$$\begin{cases} \sum_{r=1}^3 a_{r0}^C D_t^{\theta_r} u(x, y, t) - \frac{x^\alpha}{2} \frac{\partial_+^\alpha u(x, y, t)}{\partial x_+^\alpha} - \frac{y^\beta}{2} \frac{\partial_+^\beta u(x, y, t)}{\partial y_+^\beta} = f(x, y, t), & (x, y; t) \in \Omega \times (0, T], \\ u(x, y, 0) = 0, & (x, y) \in \Omega, \\ u(x, y, t) = t^3 x^2 y^2, & (x, y; t) \in \partial\Omega \times (0, T], \end{cases} \quad (6.35)$$

on the triangular domain $\Omega = \{(x, y) | 0 < x < 1, 0 < y < 1 - x\}$ with $a_1 = 2, a_2 = 0.5, a_3 = 3, \theta_1 = 0.1, \theta_2 = 0.3, \theta_3 = 0.5, \alpha = 1.5, \beta = 1.8$ and the source term

$$f(x, y, t) = \sum_{r=1}^3 \frac{6a_r t^{3-\theta_r} x^2 y^2}{\Gamma(4-\theta_r)} - t^3 x^2 y^2 \left\{ \frac{1}{\Gamma(3-\alpha)} + \frac{1}{\Gamma(3-\beta)} \right\}.$$

The exact solution is $u(x, y, t) = t^3 x^2 y^2$. We choose Multi-quadrics and Gaussian as the trial functions and report the numerical results at $t = 0.5$ in Table 6 by using $\tau = 1.0 \times 10^{-3}$. In Fig. ??, we show the used configuration of 152 nodes and its corresponding error distribution of GA-based DQ method. It can be seen that the proposed DQ methods are convergent to the exact solution as the nodal number increases.

Table 6: The numerical results at $t = 0.5$ with $q = 3, \alpha = 1.5$ and $\beta = 1.8$ for Example 6.4

M	MQ-based DQ method, $\nu = 0.3, \sigma = 1$		GA-based DQ method, $\nu = 0.5, \sigma = 1$	
	$\ u - U\ _{L^2}$	$\ u - U\ _{L^\infty}$	$\ u - U\ _{L^2}$	$\ u - U\ _{L^\infty}$
55	5.7083e-05	1.8789e-04	8.2862e-05	3.0100e-04
79	4.4719e-05	1.6652e-04	5.9078e-05	2.2586e-04
114	3.8698e-05	1.5015e-04	5.2482e-05	2.0574e-04
152	2.9558e-05	1.1855e-04	3.6037e-05	1.5203e-04

Example 6.5. Consider the two-dimensional multi-term TSFDE:

$$\begin{cases} \sum_{r=1}^3 a_{r0}^C D_t^{\theta_r} u(x, y, t) + \frac{1}{2 \cos(\alpha\pi/2)} \left(\frac{\partial_+^\alpha u(x, y, t)}{\partial x_+^\alpha} + \frac{\partial_-^\alpha u(x, y, t)}{\partial x_-^\alpha} \right) \\ \quad + \frac{1}{2 \cos(\beta\pi/2)} \left(\frac{\partial_+^\beta u(x, y, t)}{\partial y_+^\beta} + \frac{\partial_-^\beta u(x, y, t)}{\partial y_-^\beta} \right) = f(x, y, t), & (x, y; t) \in \Omega \times (0, T], \\ u(x, y, 0) = (4x^2 + y^2 - 1)^2/10, & (x, y) \in \Omega, \\ u(x, y, t) = 0, & (x, y; t) \in \partial\Omega \times (0, T], \end{cases} \quad (6.36)$$

on the elliptical domain $\Omega = \{(x, y) | 4x^2 + y^2 < 1\}$ with $a_1 = a_2 = a_3 = 1, \theta_1 = 0.6, \theta_2 = 0.7, \theta_3 = 1, \alpha = \beta = 1.6$ and the source term

$$\begin{aligned} f(x, y, t) = & \sum_{r=1}^3 \frac{a_r t^{2-\theta_r}}{5\Gamma(3-\theta_r)} x^2 (1-x)^2 y^2 (1-y)^2 \\ & + \frac{(1+t^2)}{20 \cos(\alpha\pi/2)} \left\{ (192x_l^2 + 16y^2 - 16) \frac{(x-x_l)^{3-\alpha}}{\Gamma(3-\alpha)} + \frac{388(x-x_l)^{5-\alpha}}{\Gamma(5-\alpha)} + \frac{388x_l(x-x_l)^{4-\alpha}}{\Gamma(4-\alpha)} \right. \\ & \quad \left. + (192x_r^2 + 16y^2 - 16) \frac{(x_r-x)^{3-\alpha}}{\Gamma(3-\alpha)} + \frac{388(x_r-x)^{5-\alpha}}{\Gamma(5-\alpha)} + \frac{388x_r(x_r-x)^{4-\alpha}}{\Gamma(4-\alpha)} \right\} \\ & + \frac{(1+t^2)}{20 \cos(\beta\pi/2)} \left\{ (192y_l^2 + 16x^2 - 16) \frac{(y-y_l)^{3-\alpha}}{\Gamma(3-\alpha)} + \frac{388(y-y_l)^{5-\alpha}}{\Gamma(5-\alpha)} + \frac{388y_l(y-y_l)^{4-\alpha}}{\Gamma(4-\alpha)} \right. \\ & \quad \left. + (192y_r^2 + 16x^2 - 16) \frac{(y_r-y)^{3-\alpha}}{\Gamma(3-\alpha)} + \frac{388(y_r-y)^{5-\alpha}}{\Gamma(5-\alpha)} + \frac{388y_r(y_r-y)^{4-\alpha}}{\Gamma(4-\alpha)} \right\}, \end{aligned}$$

where $x_l = -\sqrt{1-y^2}/2$, $x_r = \sqrt{1-y^2}/2$, $y_l = -\sqrt{1-4x^2}$ and $y_r = \sqrt{1-4x^2}$.

The exact solution is $u(x, y, t) = \frac{1+t^2}{10}(4x^2 + y^2 - 1)^2$. We compare the spatial accuracy of FE method and our DQ method base on Inverse Quadratics and Gaussians in term of $\|u - U\|_{L^2}$. The numerical errors at $t = 1$ of FE method [27] and DQ methods are presented in Table 5 by using $q = 2$ and $\tau = 1.0 \times 10^{-3}$. The used configurations of 112, 238 and 412 nodes, and their corresponding error distributions of IQ-based DQ method are displayed in Fig. ???. It is indicated that DQ methods produce the same error magnitude as FE method with less nodal numbers, which confirms the effectiveness of our methods.

Table 7: The comparisons of FE and DQ methods at $t = 1$ when $\theta_1 = 0.6$, $\theta_2 = 0.7$, $\theta_3 = 1$ and $\alpha = \beta = 1.6$ for Example 6.5

M	FE method [27] $\ u - U\ _{L^2}$	M	IQ-based DQ method, $\nu = 11$, $\sigma = 2$		GA-based DQ method, $\nu = 4.5$, $\sigma = 2$ $\ u - U\ _{L^2}$		$\ u - U\ _{L^\infty}$
			$\ u - U\ _{L^2}$	$\ u - U\ _{L^\infty}$	$\ u - U\ _{L^2}$	$\ u - U\ _{L^\infty}$	
70	8.6311e-03	34	7.4516e-03	1.5952e-02	6.7396e-03	1.4335e-02	
468	1.4508e-03	112	1.2389e-03	3.1296e-03	1.3671e-03	3.5605e-03	
1142	5.4919e-04	238	6.6484e-04	1.4906e-03	7.3477e-04	1.7147e-03	
1738	3.6969e-04	412	4.2034e-04	9.4854e-04	4.1947e-04	1.0285e-03	

6.3. Three-dimensional problems

Example 6.6. Consider the three-dimensional multi-term TSFDE:

$$\left\{ \begin{array}{l} 0.5{}_0^C D_t^{\theta_1} u(x, y, z, t) + 1.5{}_0^C D_t^{\theta_2} u(x, y, z, t) - \frac{(y - 0.5 + \sqrt{0.25 - (x - 0.5)^2 - z^2})^\beta}{6} \frac{\partial_+^\beta u(x, y, z, t)}{\partial y_+^\beta} \\ \qquad\qquad\qquad = f(x, y, z, t), \quad (x, y, z; t) \in \Omega \times (0, T], \\ u(x, y, z, 0) = 0, \quad (x, y, z) \in \Omega, \\ u(x, y, z, t) = (1 + t^4)(y - 0.5 + \sqrt{0.25 - (x - 0.5)^2 - z^2})^3 z^3, \quad (x, y, z; t) \in \partial\Omega \times (0, T], \end{array} \right. \quad (6.37)$$

on the sphere $\Omega = \{(x, y, z) | (x - 0.5)^2 + (y - 0.5)^2 + z^2 = 0.25\}$ with $\theta_1 = 0.3$, $\theta_2 = 0.8$ and $\beta = 1.9$. The source term is given as follows

$$f(x, y, z, t) = \left\{ \frac{12t^{4-\theta_1}}{\Gamma(5-\theta_1)} + \frac{36t^{4-\theta_2}}{\Gamma(5-\theta_2)} \right\} (y - 0.5 + \sqrt{0.25 - (x - 0.5)^2 - z^2})^3 z^3 - \frac{(1 + t^4)(y - 0.5 + \sqrt{0.25 - (x - 0.5)^2 - z^2})^3 z^3}{\Gamma(4-\beta)},$$

and the exact solution is $u(x, y, z, t) = (1 + t^4)(y - 0.5 + \sqrt{0.25 - (x - 0.5)^2 - z^2})^3 z^3$.

We choose $\tau = 1.0 \times 10^{-3}$ and report the numerical results at $t = 0.5$ in Table 8, where Multiquadratics and Reciprocal Multiquadratics are used as the trial functions. Also, we highlight the used configuration of 152 nodes and its corresponding error distribution of MQ-based DQ method in Fig. ???. The results observed illustrate that the proposed DQ methods yield the numerical solutions which are in excellent agreement with the exact solution. Moreover, the errors produced by these two DQ methods do not differ significantly under the selected discrete parameters.

7. Conclusion

In this investigation, an advanced DQ technique was developed to obtain the numerical solutions of the multi-term TSFDEs on two- and three-dimensional general domains. The considered problem was reduced into a group of multi-term fractional ODEs by extending the DQ approximation to the fractional derivatives with the help of some familiar RBFs as the trial functions. A fully discrete scheme has been derived by applying a class of high-order difference schemes to discretizing the resulting multi-term fractional ODEs. The proposed DQ scheme produces very satisfactory accuracy both in time and space, and the numerical results and comparisons with the exact solutions or the errors

Table 8: The numerical results at $t = 0.5$ with $\theta_1 = 0.3$, $\theta_2 = 0.8$ and $\beta = 1.9$ for Example 6.5

M	MQ-based DQ method, $\nu = 3$, $\sigma = 1$		RMQ-based DQ method, $\nu = 3.3$, $\sigma = 1$	
	$\ u - U\ _{L^2}$	$\ u - U\ _{L^\infty}$	$\ u - U\ _{L^2}$	$\ u - U\ _{L^\infty}$
73	1.7998e-04	8.8476e-04	1.6390e-04	8.4253e-04
101	1.2964e-04	8.0668e-04	1.2897e-04	8.1281e-04
180	5.7266e-05	4.6403e-04	5.9258e-05	4.7803e-04
336	2.1243e-05	1.3452e-04	2.2835e-05	1.4298e-04

yielded by the other methods like FE method illustrate its validity and application.

Acknowledgement: This research was supported by the projects supported by Scientific Research Fund of Hunan Provincial Education Department (Nos.19C1643, 19B509) and National Natural Science Foundations of China (No.11471262).

References

- [1] E.E. Adams, L.W. Gelhar, Field study of dispersion in a heterogeneous aquifer: 2. spatial moments analysis, *Water Res. Research* 28(12) (1992) 3293–3307.
- [2] S.N. Atluri, T. Zhu, A new meshless local petrov-galerkin (mlpg) approach in computational mechanics, *Computational mechanics* 22 (1998) 117–127.
- [3] R. Bellman, B. Kashef, E. Lee, R. Vasudevan, Differential quadrature and splines, *Computers & Mathematics with Applications* 1 (1975) 371–376.
- [4] T. Belytschko, Y.Y. Lu, L. Gu, Element-free galerkin methods, *International journal for numerical methods in engineering* 37 (1994) 229–256.
- [5] A. Bhrawy, D. Baleanu, A spectral legendre–gauss–lobatto collocation method for a space-fractional advection diffusion equations with variable coefficients, *Reports on Mathematical Physics* 72 (2013) 219–233.
- [6] A. Bhrawy, M.A. Zaky, A method based on the jacobi tau approximation for solving multi-term time–space fractional partial differential equations, *Journal of Computational Physics* 281 (2015) 876–895.
- [7] C. Çelik, M. Duman, Crank–nicolson method for the fractional diffusion equation with the riesz fractional derivative, *Journal of computational physics* 231 (2012) 1743–1750.
- [8] M. Chen, W. Deng, Fourth order difference approximations for space riemann-liouville derivatives based on weighted and shifted lubich difference operators, *Communications in Computational Physics* 16 (2014) 516–540.
- [9] A.D. Cheng, Multiquadric and its shape parametera numerical investigation of error estimate, condition number, and round-off error by arbitrary precision computation, *Engineering analysis with boundary elements* 36 (2012) 220–239.
- [10] R. Cheng, F. Sun, J. Wang, Meshless analysis of two-dimensional two-sided space-fractional wave equation based on improved moving least-squares approximation, *International Journal of Computer Mathematics* 95 (2018) 540–560.
- [11] M. Dehghan, M. Abbaszadeh, An efficient technique based on finite difference/finite element method for solution of two-dimensional space/multi-time fractional bloch–torrey equations, *Applied Numerical Mathematics* 131 (2018) 190–206.
- [12] W. Deng, M. Chen, E. Barkai, Numerical algorithms for the forward and backward fractional feynman–kac equations, *Journal of Scientific Computing* 62 (2015) 718–746.
- [13] W.H. Deng, Finite element method for the space and time fractional Fokker-Planck equation, *SIAM J. Numer. Anal.* 47 (2008) 204–226.
- [14] H. Du, M. Lim, R. Lin, Application of generalized differential quadrature method to structural problems, *International Journal for Numerical Methods in Engineering* 37 (1994) 1881–1896.
- [15] V.J. Ervin, J.P. Roop, Variational formulation for the stationary fractional advection dispersion equation, *Numer. Meth. Part. D. E.* 22 (2006) 558–576.
- [16] W. Fan, X. Jiang, F. Liu, V. Anh, The unstructured mesh finite element method for the two-dimensional multi-term time–space fractional diffusion-wave equation on an irregular convex domain, *Journal of Scientific Computing* 77 (2018) 27–52.
- [17] A. Fedoseyev, M. Friedman, E. Kansa, Improved multiquadric method for elliptic partial differential equations via pde collocation on the boundary, *Computers & Mathematics with Applications* 43 (2002) 439–455.
- [18] W. Han, X. Meng, Error analysis of the reproducing kernel particle method, *Computer methods in applied mechanics and engineering* 190 (2001) 6157–6181.
- [19] S.M. Hosseini, R. Ghaffari, Polynomial and nonpolynomial spline methods for fractional sub-diffusion equations, *Applied Mathematical Modelling* 38 (2014) 3554–3566.
- [20] C. Huang, X. Yu, C. Wang, Z. Li, N. An, A numerical method based on fully discrete direct discontinuous galerkin method for the time fractional diffusion equation, *Applied Mathematics and Computation* 264 (2015) 483–492.
- [21] J. Huang, N. Nie, Y. Tang, A second order finite difference-spectral method for space fractional diffusion equations, *Science China Mathematics* 57 (2014) 1303–1317.
- [22] J. Jia, H. Wang, Fast finite difference methods for space-fractional diffusion equations with fractional derivative boundary conditions, *Journal of Computational Physics* 293 (2015) 359–369.

[23] Y. Jiang, J. Ma, High-order finite element methods for time-fractional partial differential equations, *Journal of Computational and Applied Mathematics* 235 (2011) 3285–3290.

[24] E.J. Kansa, Multiquadraticsa scattered data approximation scheme with applications to computational fluid-dynamicslii solutions to parabolic, hyperbolic and elliptic partial differential equations, *Computers & mathematics with applications* 19 (1990) 147–161.

[25] A.A.A. Kilbas, H.M. Srivastava, J.J. Trujillo, *Theory and applications of fractional differential equations*, volume 204, Elsevier Science Limited, 2006.

[26] Y. Lin, C. Xu, Finite difference/spectral approximations for the time-fractional diffusion equation, *Journal of computational physics* 225 (2007) 1533–1552.

[27] F. Liu, L. Feng, V. Anh, J. Li, Unstructured-mesh galerkin finite element method for the two-dimensional multi-term time–space fractional bloch–torrey equations on irregular convex domains, *Computers & Mathematics with Applications* 78 (2019) 1637–1650.

[28] F. Liu, P. Zhuang, I. Turner, V. Anh, K. Burrage, A semi-alternating direction method for a 2-d fractional fitzhugh–nagumo monodomain model on an approximate irregular domain, *Journal of Computational Physics* 293 (2015) 252–263.

[29] F. Liu, P. Zhuang, I. Turner, K. Burrage, V. Anh, A new fractional finite volume method for solving the fractional diffusion equation, *Applied Mathematical Modelling* 38 (2014) 3871–3878.

[30] G.R. Liu, Y. Gu, A point interpolation method for two-dimensional solids, *International Journal for Numerical Methods in Engineering* 50 (2001) 937–951.

[31] Q. Liu, F. Liu, Y.T. Gu, P. Zhuang, J. Chen, I. Turner, A meshless method based on point interpolation method (pim) for the space fractional diffusion equation, *Applied Mathematics and Computation* 256 (2015) 930–938.

[32] M.M. Meerschaert, C. Tadjeran, Finite difference approximations for fractional advection-dispersion flow equations, *J. Comput. Appl. Math.* 172(1) (2004) 65–77.

[33] D.A. Murio, Implicit finite difference approximation for time fractional diffusion equations, *Computers & Mathematics with Applications* 56 (2008) 1138–1145.

[34] B. Nayroles, G. Touzot, P. Villon, Generalizing the finite element method: diffuse approximation and diffuse elements, *Computational mechanics* 10 (1992) 307–318.

[35] G. Pang, W. Chen, K. Sze, Gauss–jacobi-type quadrature rules for fractional directional integrals, *Computers & Mathematics with Applications* 66 (2013) 597–607.

[36] G. Pang, W. Chen, K. Sze, Differential quadrature and cubature methods for steady-state space-fractional advection-diffusion equations, *Comput. Model. Eng. Sci.* 97 (2014) 299–322.

[37] S. Qin, F. Liu, I.W. Turner, A 2d multi-term time and space fractional bloch-torrey model based on bilinear rectangular finite elements, *Communications in Nonlinear Science and Numerical Simulation* 56 (2018) 270–286.

[38] L. Qiu, W. Deng, J.S. Hesthaven, Nodal discontinuous galerkin methods for fractional diffusion equations on 2d domain with triangular meshes, *Journal of Computational Physics* 298 (2015) 678–694.

[39] J. Ren, Z.Z. Sun, X. Zhao, Compact difference scheme for the fractional sub-diffusion equation with neumann boundary conditions, *Journal of Computational Physics* 232 (2013) 456–467.

[40] W. Tian, H. Zhou, W. Deng, A class of second order difference approximations for solving space fractional diffusion equations, *Mathematics of Computation* 84 (2015) 1703–1727.

[41] Y. Wu, C. Shu, Development of rbf-dq method for derivative approximation and its application to simulate natural convection in concentric annuli, *Computational Mechanics* 29 (2002) 477–485.

[42] Z. Yang, Z. Yuan, Y. Nie, J. Wang, X. Zhu, F. Liu, Finite element method for nonlinear riesz space fractional diffusion equations on irregular domains, *Journal of Computational Physics* 330 (2017) 863–883.

[43] S.B. Yuste, Weighted average finite difference methods for fractional diffusion equations, *Journal of Computational Physics* 216 (2006) 264–274.

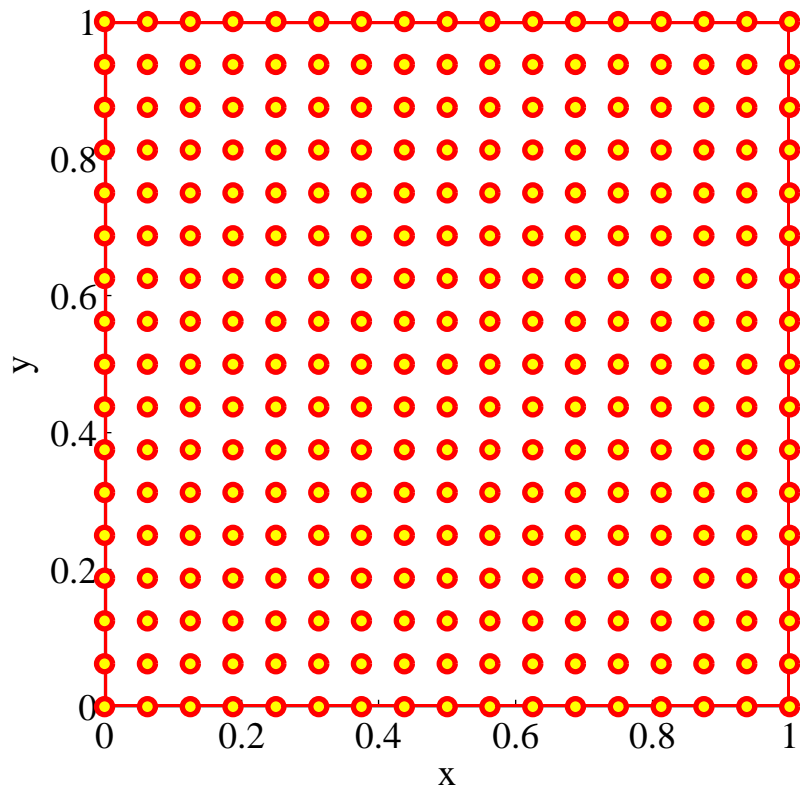
[44] F. Zeng, F. Liu, C. Li, K. Burrage, I. Turner, V. Anh, A crank–nicolson adi spectral method for a two-dimensional riesz space fractional nonlinear reaction-diffusion equation, *SIAM Journal on Numerical Analysis* 52 (2014) 2599–2622.

[45] H. Zhang, F. Liu, V. Anh, Galerkin finite element approximations of symmetric space fractional partial differential equations, *Appl. Math. Comput.* 217 (2010) 2534–2545.

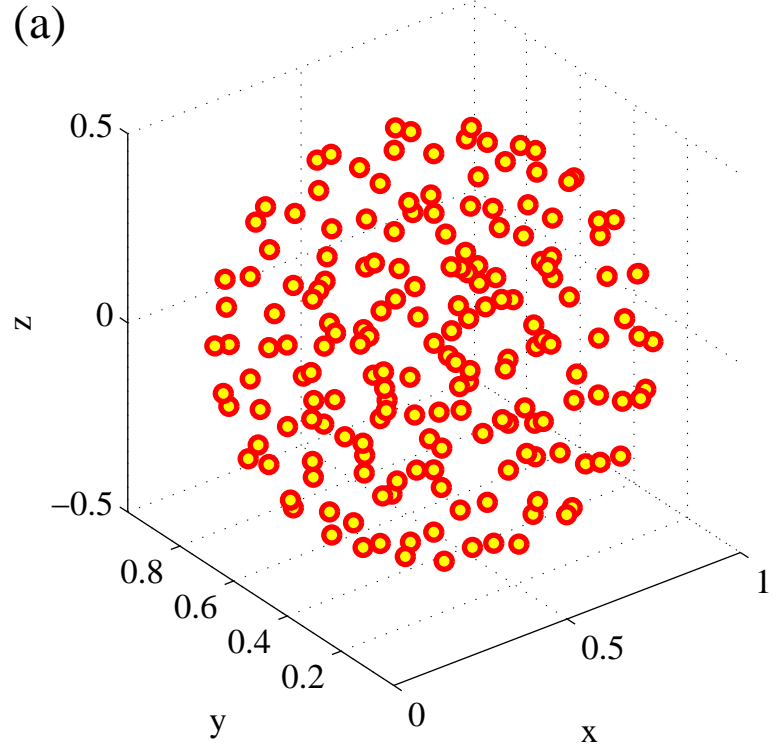
[46] J. Zhang, G. Yan, Lattice boltzmann method for the fractional sub-diffusion equation, *International Journal for Numerical Methods in Fluids* 80 (2016) 490–507.

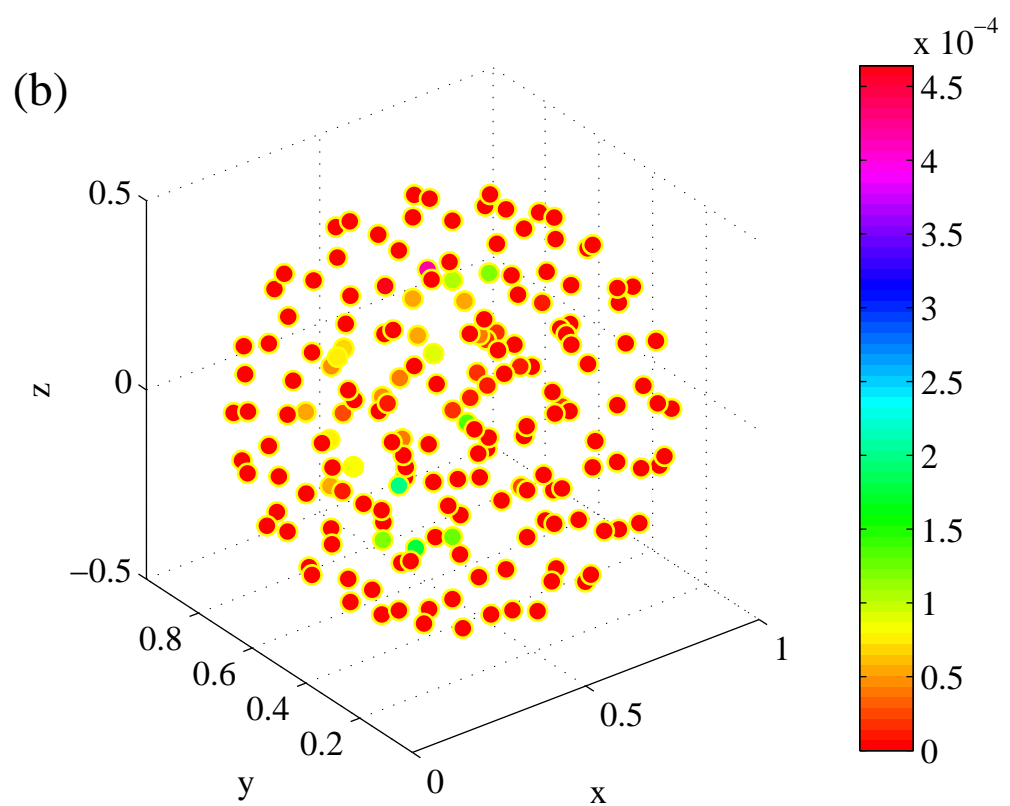
[47] X. Zhu, Y. Nie, J. Wang, Z. Yuan, A numerical approach for the riesz space-fractional fisher’equation in two-dimensions, *International Journal of Computer Mathematics* 94 (2017) 296–315.

(a)

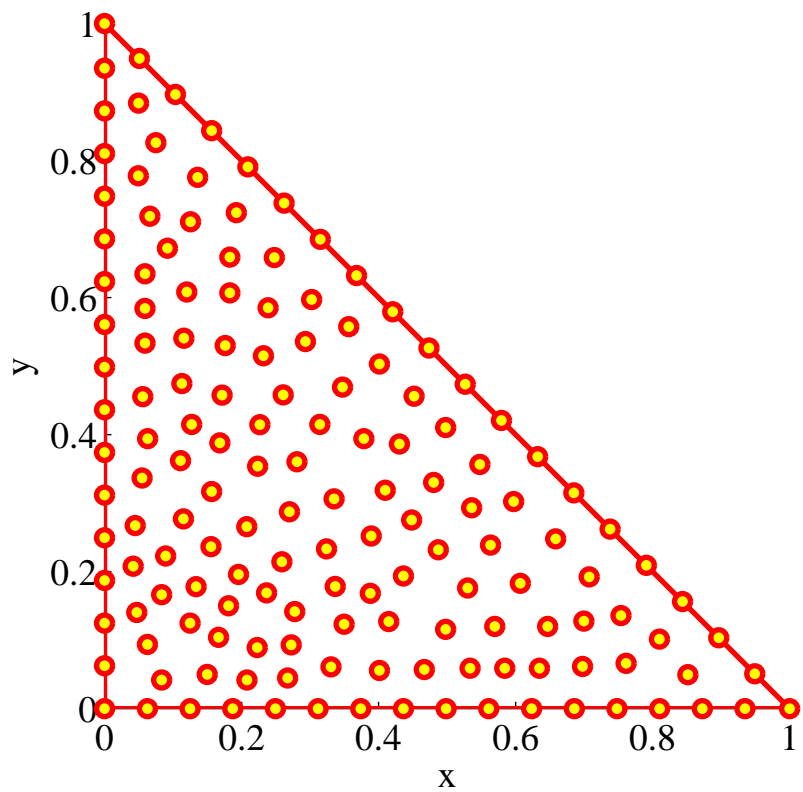


(a)

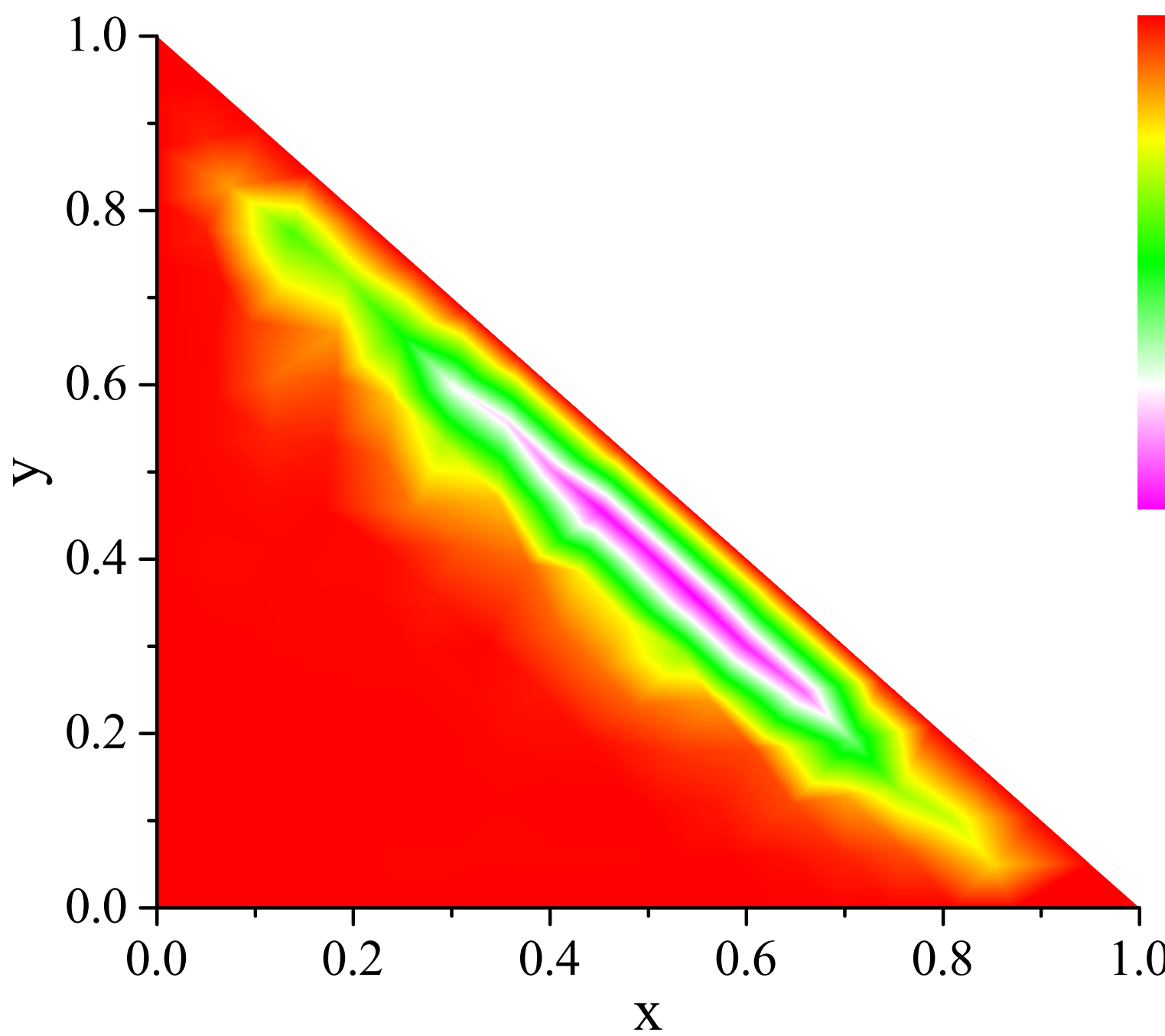




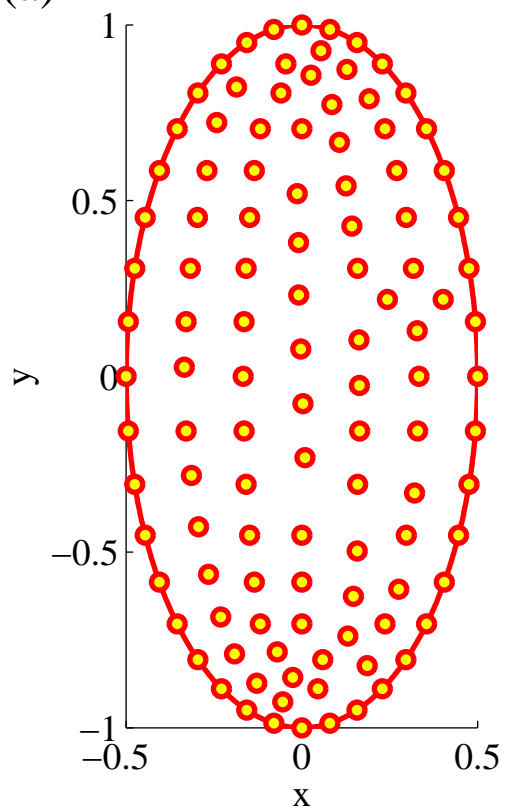
(a)



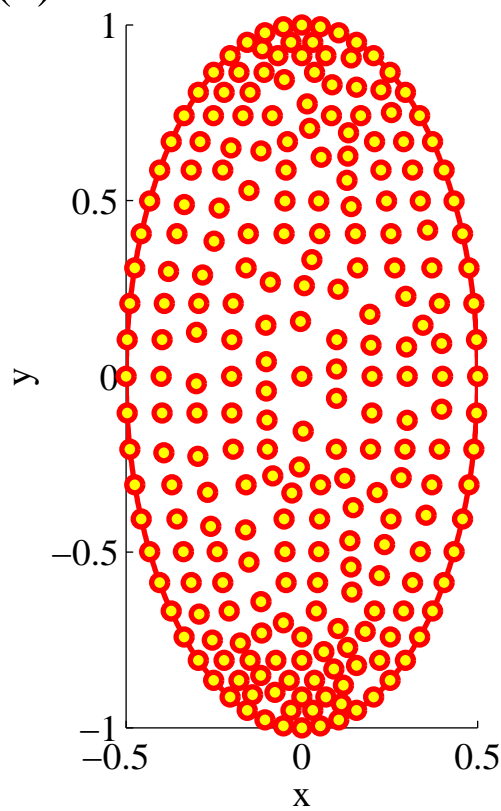
(b)



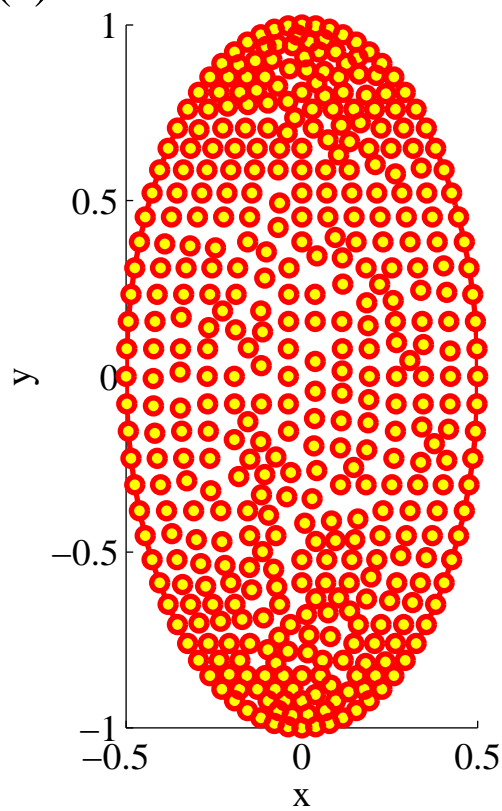
(a)



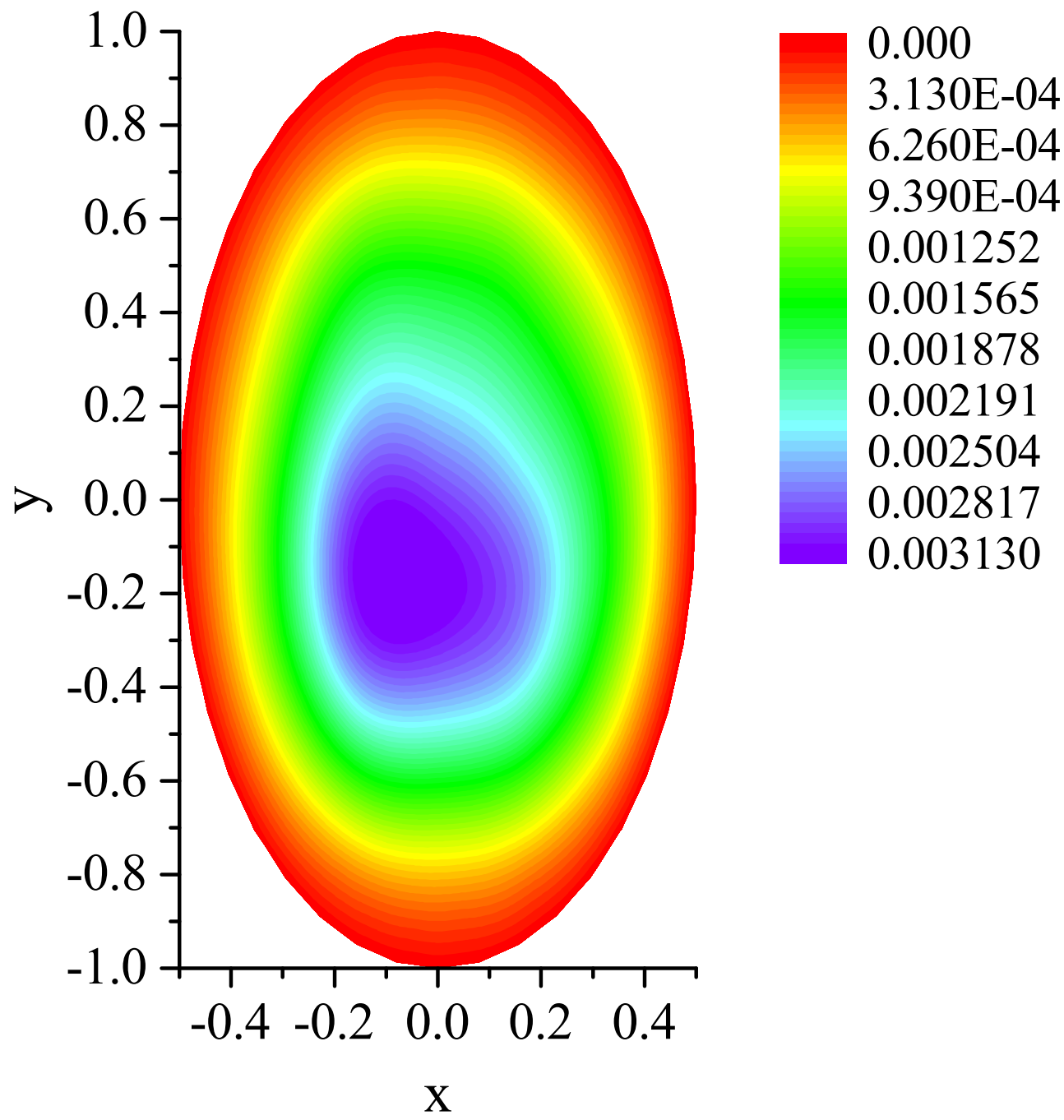
(b)



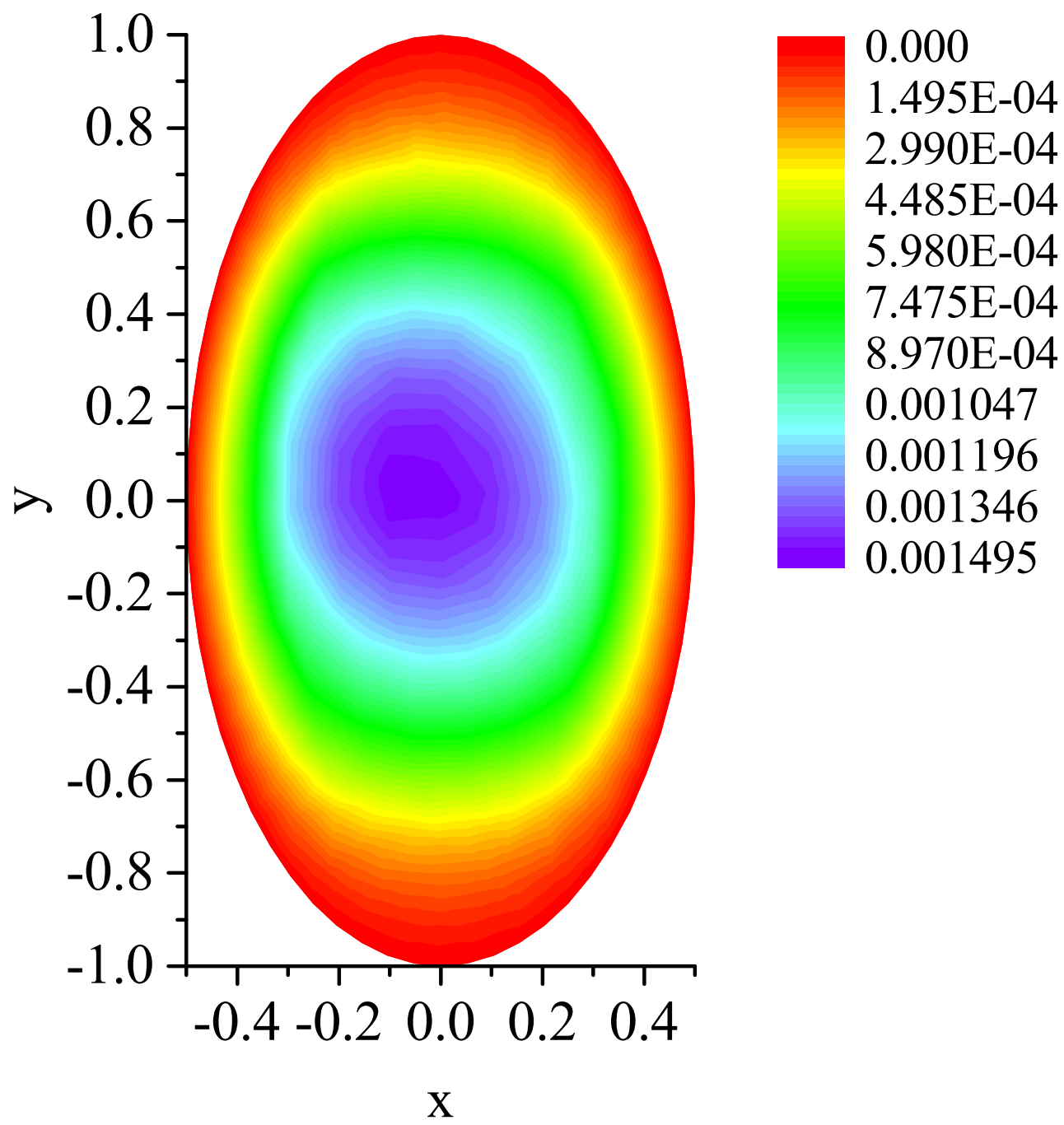
(c)



(d)



(e)



(f)

